Optics & Laser Technology 43 (2011) 1436–1441

Contents lists available at ScienceDirect

Optics & Laser Technology

journal homepage: www.elsevier.com/locate/optlastec

Designing high performance Er^{+3}-doped fiber amplifier in triangular-lattice photonic crystal fiber host towards higher gain, low splice loss

Kajal Mondal, Partha Roy Chaudhuri *

Department of Physics and Meteorology, Indian Institute of Technology Kharagpur-721302, India

ARTICLE INFO

Article history:
Received 26 November 2010
Received in revised form
1 April 2011
Accepted 21 April 2011
Available online 5 May 2011

Keywords:
Triangular-lattice PCF
EDFA
Splice losses

ABSTRACT

In order to improve the over-all performance of all-fiber amplifier using Er^{+3}-doped triangular-lattice photonic crystal fiber (PCF), we performed a detailed study on the amplifying characteristics of the PCF host by varying all associated geometrical parameters towards utilizing controllable effective numerical aperture and tight modal confinement. A finite difference (FD) mode convergence analysis is used to determine the modal propagation characteristics of the structure, which is then used to solve a standard *propagation and population rate equation*. Our results show that a spectral gain of the amplifier as high as 51 dB and that too over a short length ~2.5 m of the fiber is achievable by optimizing the transverse geometry of the fiber. Aimed at field-deployment of the amplifier as inline component, we calculate the important all-fiber characteristics, namely, beam divergence, bending loss and nonlinearity and then optimize the splicing/coupling loss (resulting from the fundamental mode mismatch only) of this active fiber device. Notably, the splice loss with standard telecom-grade SMF-28 fiber is considerably minimized through an improved mode-matching of the design. These results record a marked improvement in fiber amplifier research in realizing high-performance EDFA-PCF amplifiers.

© 2011 Elsevier Ltd. All rights reserved.

1. Introduction

The photonic crystal fiber technology has offered a versatile and powerful platform to realize fibers and inline components with many exciting propagation characteristics, which are far beyond the ones achievable through the simple core-cladding approach [1,2]. The most useful attributes of PCFs are the high index-contrast [3] between silica and air, and a highly flexible design of fiber geometry in terms of *size*, *shape* and *arrangement of air-holes* in the cladding structure [4,5]. The high index-contrast enables one to design fibers with large effective numerical aperture [6] over a small core dimension (of the order of wavelength) and hence a very tight modal confinement [7] as required by an amplifier host. In addition, the average index-guiding effect [4] in PCF with an appropriate *filling fraction* makes it possible to achieve a largely tailorable mode-field area over a useful single-mode regime [8], which is an important requirement for controllable laser power delivery as well as for reducing splice/coupling loss. Also, the effective mode-field-diameter (MFD) for the pump (λ_p) and signal (λ_s) wavelengths can be made to control the associated overlap for ready positioning of the pump and signal fields across the active region. These have made PCF an attractive member of active fiber and all-fiber amplifier devices. Erbium (Er) and Ytterbium (Yb) are the two most suitable active dopants in the silica host, and a few works – both analysis and experimental demonstrations of Yb [9,10] and Er-doped [11,12] PCF-based amplifiers – have appeared in the literature. However, a huge flexibility in designing with many unusual guiding features of PCF tempted us to revisit the analysis exercise for a maximum utilization of these properties.

In this work, the gain properties of Er^{+3}-doped triangular-lattice photonic crystal fibers are investigated extensively by analyzing the effect of PCF geometry with the dopant radius in the core. We have used a finite difference field convergence technique [13,14] for mode calculation, which is combined with a standard *population and propagation rate equation-solving algorithm*. By varying PCF geometry, we have optimized [15] the pump and signal beam overlap, and a converged design has been established, which exhibits an amplifier gain as good as 51 dB using a PCF length as short as 2.5 m. As an important requirement, the splice loss of the PCF amplifier [16] with standard telecommunication fiber (SMF-28) has been minimized through an adjustment of mode-field area keeping the gain characteristics unaffected. Such a fiber's performance is usually limited by bend-induced loss caused by small effective index-contrast at shorter wavelengths [17]. However, our studies exhibit a less bending sensitivity of the designed PCF as compared to conventional fibers [18].

2. Design analysis

Designing and analyzing the fiber amplifier's characteristics primarily owe to a precise calculation of the propagating

* Corresponding author. Tel.: +91 3222 283842; fax: +91 3222 255303.
E-mail address: roycp@phy.iitkgp.ernet.in (P.Roy Chaudhuri).

0030-3992/$ - see front matter © 2011 Elsevier Ltd. All rights reserved.
doi:10.1016/j.optlastec.2011.04.015

electromagnetic field distribution across the cross-section of the host fiber. The efficiency of the amplifier is a direct outcome of the overlap of modal fields associated with the signal and pump beams within the doped area. Then, PCF is largely to look for the geometry where this overlap is strongest for a given size of the active region. In our analysis, we considered triangular-lattice PCF geometry, and for calculation of the mode-field distributions, a finite difference mode convergence recipe [13,14] has been implemented. Using the definitions of mode effective area (A_{eff}) [19] for PCFs as well as considering an equivalent modal spot-size, we evaluate the overlap integrals for the pump and signal wavelengths.

The mode-field distribution and mode effective index are the two key parameters in describing all important properties of guided modes. In PCF, these parameters largely depend on the kind of transverse structure associated [20]. We calculate the mode effective area and hence the modal spot-size following our mode-analysis method. The effective area of the modal field is then determined taking surface integral of transverse electric field (E_t) along the whole cross-section of the triangular-lattice PCF [19]

$$A_{\text{eff}} = \frac{\left[\iint_s |E_t|^2 dx\,dy\right]^2}{\iint_s |E_t|^4 dx\,dy}. \quad (1)$$

The modal spot-size (r_{mod}) is then calculated ($A_{\text{eff}}=\pi r_{\text{mod}}^2$) from A_{eff} at the required signal wavelength, which is the new input data to the *population and propagation rate equations*.

3. Numerical results and discussion

In this section, we discuss our results namely, gain properties [21], noise characteristics, splice loss, nonlinearity, beam divergence and finally, prescribe an efficient design of a PCF amplifier.

3.1. Gain properties

The gain of a fiber amplifier depends on the emission and absorption cross-section of active-ion transitions and opto-geometric parameters. As an initial step of analysis, we consider the fiber studied in [22]. The fiber is a triangular-lattice PCF (the ideal structure is shown in Fig. 1) and it has the following geometrical parameters: air-hole diameter, $d=1$ μm, pitch, $\Lambda=2$ μm such that d/Λ of the PCF is 0.5. Following the work reported in [23], in our analysis, we take the erbium-ion concentration as $\sim 2.6\times10^{25}$ ions/m^3 and assume that the erbium ions occupy a region of 0.5 μm radius at the center of the PCF core, pumped by a backward pump at 0.98 μm wavelength of power (P_p) 225 mW. Thus initially we attempt to reproduce the quoted results [23] using the given condition of the PCF host with doped length (L_F) as 5.5 m and we notice a good agreement with the reported results. The results are plotted in Fig. 2, which clearly suggest that the obtainable maximum gain of EDFA-PCF amplifier can be made above 51 dB at 1.535 μm wavelength of signal light. The corresponding set of PCF-EDFA parameters that we consider in this plot are summarized in Table 1. In the following sections, we detail our series studies on how the variations of *air-hole diameter*, *pitch*, *doping radius*, *pump power* and *input signal power* (P_s) of PCF amplifier influence the gain at the desired communication wavelengths around 1.55 μm. Hence the *optimization of fiber length* is achieved without any reduction of the obtainable maximum gain of the amplifier at this wavelength.

3.1.1. Air-hole diameter and pitch dependence

The mode effective area, i.e., field-confinement inside the core of PCF has a direct influence on the amplifier gain properties [24] because of its overlap with the active dopant ions across this region. The A_{eff} of the PCF can be tuned by changing the size and position of the air-holes within the cladding structure to look for a maximum overlap under suitable pumping condition and hence the maximum gain. Fig. 3 shows the gain as a function of active length of the PCF by varying d between 1.0 and 0.6 μm keeping the doping radius (r_d) fixed at 1.0 μm and Λ at 2 μm (i.e. r_d/Λ is 0.5). The variation therefore shows d/Λ (marked in the inset) dependence of the gain. As evident, the amplifier gain saturates beyond a certain length of the doped-PCF thereby defining the minimum active length of this PCF required to achieve the maximum level of amplification. The corresponding minimum length is termed as optimum length (L_{opt}). The figure also indicates that optimum length decreases with increase in d

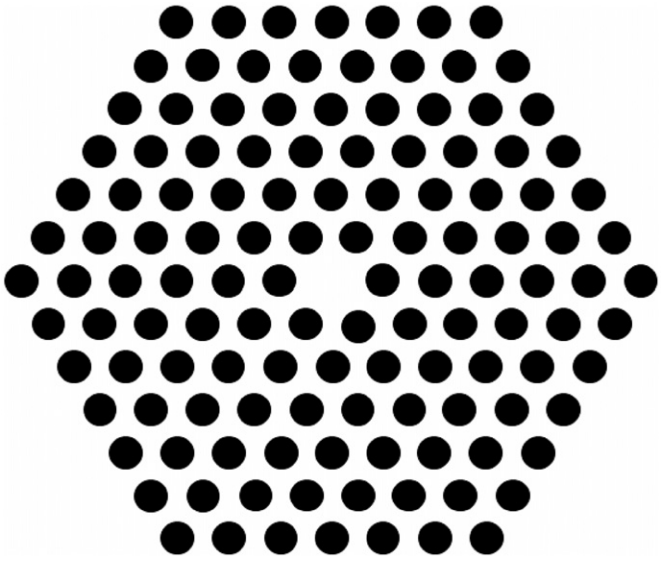

Fig. 1. Simulated ideal PCF structure considered as amplifier host.

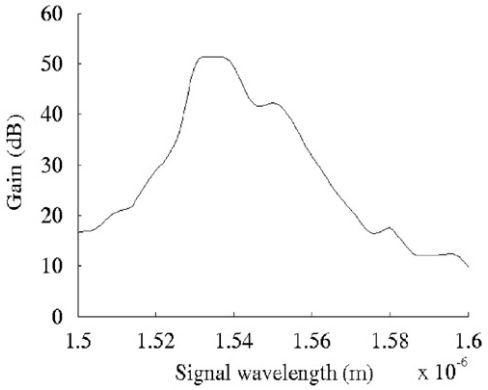

Fig. 2. Calculated spectral gain of the PCF-based erbium doped fiber amplifier studied initially with parameters listed in Table 1.

Table 1
EDFA-PCF parameters that have been used for the initial step of evolution.

Parameters	Symbol	Value
Pump power (mW)	P_p	225
Pump wavelength (μm)	λ_p	0.98
Signal power (μW)	P_s	1
Fiber length (m)	L_F	7.8
Doping radius (μm)	r_d	0.5
Doping concentration (ions/m^3)	ρ	2.6×10^{25}
Hole diameter (μm)	d	1
Pitch (μm)	Λ	2

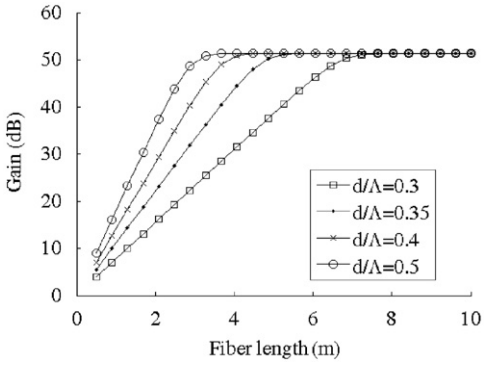

Fig. 3. Gain as a function of doped-PCF length for different d values with $\Lambda=2$ μm and $r_d/\Lambda=0.5$.

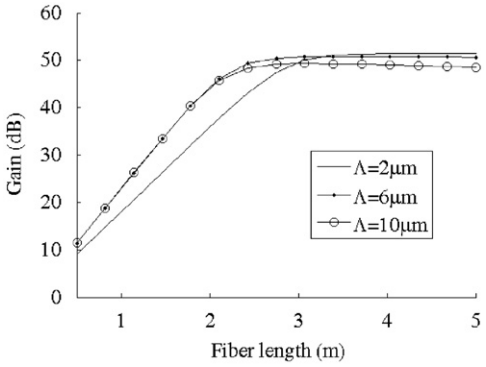

Fig. 4. Gain Vs doped-PCF length for different Λ values with $d/\Lambda=0.5$ and $r_d/\Lambda=0.5$.

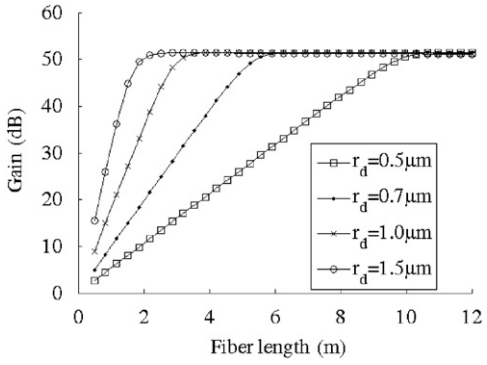

Fig. 5. Calculated amplifier gain as a function of fiber length for various doping radii at the core.

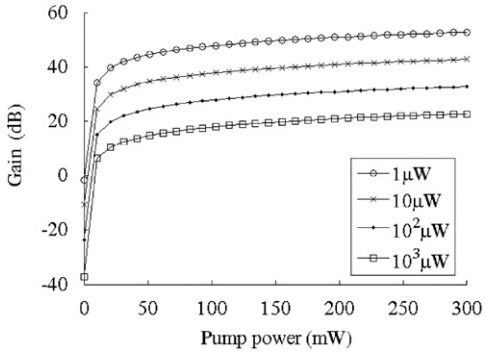

Fig. 6. Gain variation as a function of pump power for different signal power ($L_F=7.8$ m and $r_d/\Lambda=0.5$).

(or d/Λ, as Λ is fixed). For example, L_{opt} was 7.7 m having a maximum gain of 51.29 dB when d/Λ was 0.3 but it is reduced to 4.13 m having a maximum gain of 51.4 dB when d/Λ is 0.5. So, in the above variation the maximum gain remains almost constant although the L_{opt} decreases. We have observed this property till the value of Λ reaches 10 μm. Also, dependence of gain on the air-hole diameter is seen to remain same for every value of Λ. The only difference observed is that for the higher value of Λ, the maximum obtainable gain and L_{opt} decrease in comparison with that for lower value of Λ. However, the maximum gain remains above 50 dB for Λ below 8 μm. In Fig. 4, we have plotted gain as a function of doped fiber length for different Λ value indicated in the figure, keeping d/Λ at 0.5. Here, we have noticed that maximum gain and L_{opt} reduced to 49.3 dB and 3.1 m, respectively, at $\Lambda=10$ μm.

3.1.2. Doping radius dependence

To study the variation of doping radius, r_d with L_F, r_d is varied in the range of 0.5–1.5 μm, keeping the other parameters (e.g. P_p, λ_p, P_s, ρ, d and Λ) unchanged as used in the initial step. The results of this study are plotted in Fig. 5. It shows that the L_{opt} decreases considerably as a function of increase in radius of doped region. However, the maximum gain remains the same in this case. For example, a gain of 51.4 dB is obtained with only 3.0 m long doped-PCF for $r_d=1.5$ μm. This finding will be useful for reducing the L_{opt} by increasing the doping radius, r_d. In this optimization one should take care that increasing the doping radius would cause a corresponding decrease in maximum obtainable gain. This resulting reduction in maximum obtainable gain is seen to decrease considerably for high Λ values. We have observed the gain properties for various d and Λ combinations discussed above by varying r_d between 0.25Λ and 0.75Λ. Within this range of r_d the maximum gain does not remain above 51 dB for the value of Λ beyond 7 μm.

3.1.3. Effect of pump power

Pump power is another important parameter to control the gain characteristics of a fiber amplifier. Here, we have estimated the effect of pump power on amplifier gain. The calculated results are depicted in Fig. 6, which shows the dependence of gain on the pump power for input signal of different powers (shown in the inset) at wavelength 1.55 μm. In this calculation, we have considered a triangular-lattice doped-PCF with $r_d/\Lambda=0.5$ keeping the other parameters (e.g. L_F, λ_p, ρ, d and Λ) same as given in Table 1. Initially, at a meta-stable state, the stimulated carriers increase the population till saturation is achieved. For that reason, at first the gain increases linearly with the pump power and eventually it gets saturated. Here the increase in input signal power causes the decrease in saturation gain, which depends on the ratio of output and input signal power. This study is very important for minimization of pump power, which tells us the minimum pump power required to obtain the maximum gain. However, for 1 μW signal power, 51 dB gain can be achieved by pump power ~225 μW with the above-mentioned configuration.

3.1.4. Effect of input signal power

Next, we have explored the results of input signal power on the gain of PCF amplifier [25]. Here, we have observed the gain properties by determining the output signal power due to various input signal power keeping the other parameters (e.g. L_F, r_d, P_p, λ_p, ρ, d and Λ) same as the initial step of evolution given in Table 1. The results of these calculations are depicted in Fig. 7, where the

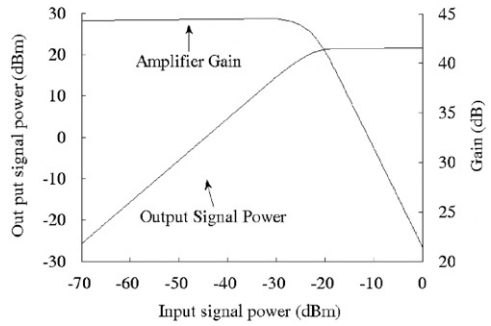

Fig. 7. Output signal power and gain as a function of input signal power (L_F=7.8 m and r_d=0.5 μm).

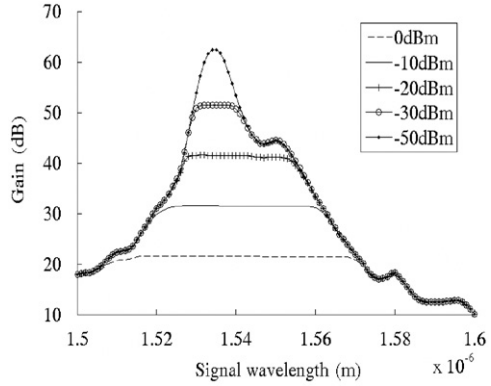

Fig. 8. Gain spectrum at different input signal power (L_F=7.8 m and r_d=0.5 μm).

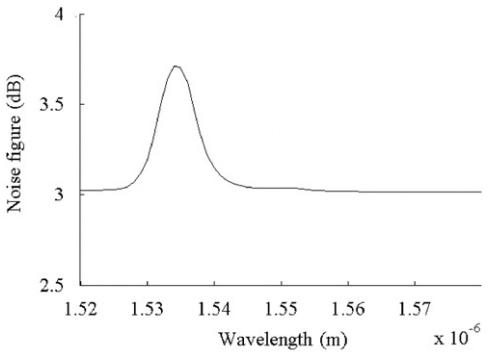

Fig. 9. Noise characteristics of the amplifier as estimated from the amplifier analysis.

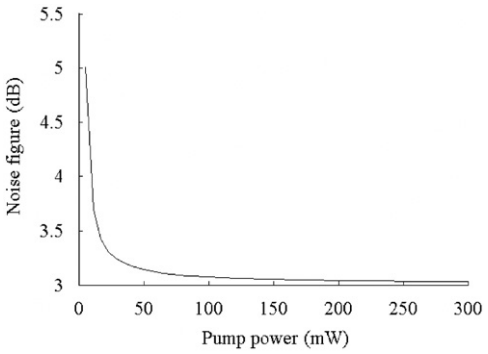

Fig. 10. Dependence of noise figure on pump power.

output signal power and gain are plotted as a function of the input signal power. As the power of input signal increases, the stimulated carriers make more and more transitions thereby increasing the output power so that, the amplifier maintains constant gain. Further increase in input signal power, decreases the population inversion, which drops the gain. However, eventually a saturation point is reached at which the output power does not improve, but the gain becomes less due to increase in input power. In this process, a limiting value of saturation input signal power is achieved ~ -30 dBm (1 μW). Throughout the study, we have used this value of input signal power, which gives the maximum efficiency. However, the calculated value of the saturation gain 42 dB, which is less than the earlier obtained value of gain 51 dB, is achievable by length adjustment. The spectral gain at different input signal power is shown in Fig. 8 where, gain remains constant at its maximum within a certain range of input wavelength. This range of input wavelength is called gain bandwidth of the amplifier, which decreases with increase in gain [25] at a lower value of input signal power.

3.2. Noise characteristics

Signal through an optical amplifier is amplified mainly due to stimulated emission. But there is also possibility of spontaneous emission from higher energy state along with stimulated emission. This spontaneous emission is completely incoherent with respect to input signal beam and propagates in both forward and backward directions. Part of the radiation due to spontaneous emission is coupled with the LP_{01} mode of the fiber and, as it propagates through the structure, amplification takes place just like the signal beam. This radiation, the *amplified spontaneous emission* (ASE), results in the generation of noise within the amplifier. Here we consider the noise figure (NF) of an amplifier, which is the ratio of signal to noise ratio $(SNR)_i$ at the input to that at the output $(SNR)_o$. For high-gain amplifier NF is defined as

$$NF = 2\left(\frac{n_s N_2}{n_s N_2 - N_1}\right), \tag{2}$$

where n_s, N_2 and N_1 are, respectively, the ratio of signal emission cross-section to signal absorption cross-section, upper state population and lower state population density. The calculated noise signatures of the Er^{+3}-doped triangular PCF amplifier are shown in Figs. 9 and 10. In Fig. 9 we plot the NF of 5 m long PCF in the signal wavelength range of 1.52–1.58 μm where the other parameters (e.g. r_d, P_s, P_p, λ_p, ρ, d and Λ) correspond to those given in Table 1. Fig. 10 shows the calculated NF variation with input pump power in the range of 5–300 mW at signal wavelength 1.55 μm using the above configuration. Clearly, minimization of pump power also does not increase the noise figure much. The important point regarding this study is that NF is not going below the quantum limit (3 dB).

3.3. Other important parameters: nonlinearity, beam divergence and splice loss

When deployed as communication/signal processing components, it is important to quantify other essential parameters for all-fiber devices, namely splice loss, beam divergence, numerical aperture and nonlinearity coefficient. While optimizing amplifying features of the fiber, we have also evaluated the aforesaid parameters of the holey fiber under investigation. A high value of nonlinearity coefficient of 19.7 W km^{-1} and low beam divergence of 0.31 rad are obtained at 1.55 μm light wavelength where the numerical aperture is seen to remain unvaried for different light wavelength starting from 0.8 to 2.1 μm. Also, the PCF shows a micro-bending loss less than that exhibited by a conventional

single-mode fiber [26]. However, in this phase, we stressed more investigation on the variation of splicing loss (loss occurrence due to modal mismatch between two adjacent fibers), an unavoidable feature in long-haul communication, compared to other important parameters of a fiber. This might impose a severe limitation on commercialization of EDFA-PCF since the modal confinement of PCF is much more compared to any other conventional fiber. There are many sources, which introduce loss at the splice point including the method of splicing. However, in this phase, we have investigated the variation of splicing loss that occurs due to *fundamental mode mismatch* only. Many researchers have shown that high gain values can be easily obtained with erbium doped PCFs [23,27]. That is why it is the most important aspect of our design purpose to reduce the coupling loss between the triangular PCF and a conventional single-mode fiber. Therefore, as a typical result, we discuss here coupling loss minimization of the PCF with standard SMF through minimized mode mismatch. The splice loss has been calculated with the help of the formulae proposed in [16] and all the results are depicted in Fig. 11 along with a table (see Table 2). In order to minimize splice loss, first we analyze a triangular PCF with $d/\Lambda=0.5$, and between $\Lambda=2$ and 10 μm. This result suggests that by adjusting the pitch a little higher (~7 μm) we can reduce the resulting splice loss. But a continued increase in Λ, however, makes the PCF eventually multi-mode [28]. Hence, we have reduced d/Λ from 0.5 to 0.3 through 0.4 and 0.35. We have observed the splice loss for Λ in the range 2–10 μm. Typically, for $d/\Lambda=0.4$, the splice loss varies from 4.012 dB when $\Lambda=2$ μm to only 0.0006 dB when $\Lambda=7$ μm. For $d/\Lambda=0.35$, the splice loss varies from 3.099 dB when $\Lambda=2$ μm to 0.013 dB when $\Lambda=7$ μm. According to the earlier discussion both the above d/Λ values (0.35 and 0.4) and Λ within the range of 2–7 μm exhibit almost same gain dependence on fiber length when r_d was varied from 0.25Λ to 0.75Λ. Since the structure then becomes leaky and bend sensitive, a trade-off between d/Λ and bending loss prescribes a suitable design of the PCF-EDFA. The results depicted in Fig. 11 shows that splice losses decrease around a pitch value around 7 μm [29], which is because triangular PCF with $\Lambda=7$ μm has a mode-field-diameter quite similar to that of an SMF-28 [30].

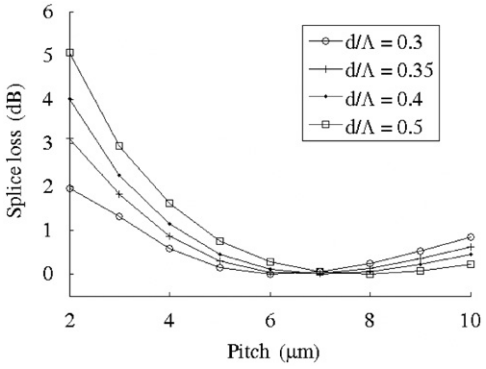

Fig. 11. Splicing loss between designed PCF with a standard SMF-28.

Table 2
Calculated splice losses of the PCF with SMF-28™ for different pitch with d/Λ as a parameter considering only the fundamental mode mismatch.

d/Λ	0.5		0.4		0.35		0.3	
Λ (μm)	2	8	2	7	2	7	2	6
Splice loss (dB)	5.068	0.0013	4.012	0.0006	3.099	0.013	1.95	0.0019

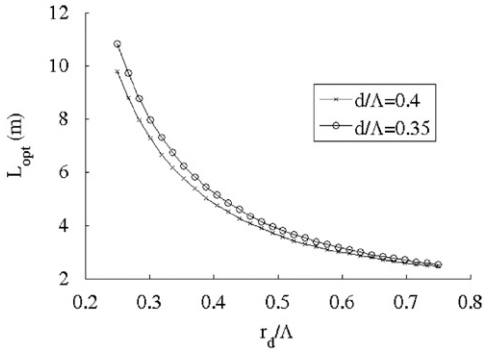

Fig. 12. Variation of optimum fiber length with r_d/Λ.

Table 3
Converged set of optimized values of the amplifier parameters (given in Table 1) for maximum gain, minimum doped-PCF length and low splice loss.

Parameters	Symbol	Value
Pitch (μm)	Λ	7
Hole diameter (μm)	d	0.4Λ
Fiber length (m)	L_F	2.5
Doping radius (μm)	r_d	0.75Λ

3.4. Optimization of fiber length

Next we go for the final optimization of length of the PCF at the above-mentioned designing parameters, i.e., $d/\Lambda=0.35$ and also $d/\Lambda=0.4$ having $\Lambda=7$ where the fiber shows single-mode operation. As discussed earlier, these parameters are convenient in order to achieve low splice loss and less L_{opt} without affecting the maximum obtainable gain. Since the dopant radius controls the optimum length, converging to these parameters of the PCF towards a design, we then fine-tune our optimization by tailoring the effect of dopant radius on the amplifier gain. We studied this effect for the dopant radii r_d in the range of $0.25–0.75\Lambda$, beyond which the maximum obtainable gain tends to decrease. The results are shown in Fig. 12. Clearly, this figure indicates that L_{opt} decreases with increase in r_d and $r_d=0.75\Lambda$ we obtain L_{opt} as short as 2.5 m. Therefore, in summary, an amplifier gain of more than 51 dB can be obtained with 2.5 m long erbium doped, single-mode PCF with considerably reduced splice loss. The converged set of parameters is given in Table 3.

4. Conclusion

Fiber amplifiers are inline active devices, which form essential elements in signal processing nodes of optical networks. In this research, we performed a thorough design analysis of erbium doped fiber amplifier based on triangular-lattice holey fiber and the work is detailed in this article. The analysis teaches us how the gain and noise performance of the amplifier are influenced by various PCF parameters as well as amplifiers' input conditions. By utilizing the strong confinement properties of PCF, we have maximized the spectral gain of the amplifier to a value above 51 dB with a corresponding minimized fiber length of 2.5 m. Through our analysis methodology, we have studied several other important parameters inherently associated with all-fiber systems in communication, namely, beam divergence, nonlinearity and splicing loss. Splicing loss between the designed PCF amplifier and a standard SMF-28 is reduced to a bare minimum value at the optimum fiber geometry. The research summarily provides a comprehensive understanding about of the influence of various

parameters on the gain and noise spectra of PCF-based fiber amplifier.

Acknowledgment

The authors sincerely acknowledge the Department of Science and Technology (**DST**), Govt. of India, and Defence Research and Development Organisation (**DRDO**), Govt. of India for the financial support to carry out this study.

References

[1] Russell PStJ, Knight JC, Birks TA, Cregan RF, Mangan BJ, De Sandro JP. Photonic crystal fibres. In: Proceedings of the ECOC 97; 1997, p. 63–4.
[2] Roy S, Roy Chaudhuri P. Supercontinuum generation in visible to mid-infrared region in square-lattice photonic crystal fiber made from highly nonlinear glasses. Opt Commun 2009;282:3448–55.
[3] Monro TM, Bennett PJ, Broderick NGR, Richardson DJ. Holey fibers with random cladding distributions. Opt Lett 2000;25:206–8.
[4] Hansen TP, Broeng J, Libori SEB, Knudsen E, Bjarklev A, Jensen JR, et al. Highly birefringent index-guiding photonic crystal fibers. IEEE Photon Technol Lett 2001;13:588–90.
[5] Roy S, Mondal K, Roy Chaudhuri P. Modeling the tapering effects of fabricated photonic crystal fiber and tailoring birefringence, dispersion, and supercontinuum generation properties. Appl Opt 2009;48:G106–13.
[6] Mortensen NA, Folken JR, Skovgaard Peter MW, Broeng J. Numerical aperture of single-mode photonic crystal fibers. IEEE Photon Technol Lett 2002;14:1094–6.
[7] Monro TM, Richardson DJ, Broderick NGR, Bennett PJ. Holey optical fibers: an efficient modal model. J Lightwave Technol 1999;17:1093–102.
[8] Mortensen NA, Nielsen MD, Folkenberg JR, Petersson A, Simonsen HR. Improved large mode-area endlessly single-mode photonic crystal fibers. Opt Lett 2003;28:393–5.
[9] Yan L, Chunyu W, Yutian L. A four-passed ytterbium doped fiber amplifier. Opt Laser Technol 2007;39:11–114.
[10] Limpert J, Liem A, Reich M, Schreiber T, Nolte S, Zellmer H, et al. Low-nonlinearity single-transverse-mode ytterbium-doped photonic crystal fiber amplifier. Opt Express 2004;12:1313–9.
[11] Harun SW, Ahmad H. Low noise double pass L-band erbium-doped amplifier. Opt Laser Technol 2004;36:245–8.
[12] Sánchez-Martín José A, Rebolledo Miguel Ángel, Álvarez José Miguel, Vallés Juan A, Díez Antonio, Andrés Miguel V. Erbium-doped-silica photonic crystal fiber characterization method: description and experimental check. IEEE J Quantum Electron 2010;46:1145–52.
[13] Roy Chaudhuri P, Ghatak AK, Pal BP, Lu C. Fast convergence and higher-order calculation of optical waveguides: perturbation method with finite difference algorithm. Opt Laser Technol 2005;37:61–7.
[14] Roy Chaudhuri P, Roy S. Determining properties of fabricated index-guiding photonic crystal fibers using SEM micrograph and mode convergence algorithm. J Lightwave Technol 2008;26:379–86.
[15] Jiang C, Zeng Q. Optimization of erbium-doped waveguide amplifier. Opt Laser Technol 2004;36:167–71.
[16] Chong JH, Rao MK. Development of a system for laser splicing photonic crystal fiber. Opt Express 2003;11:1365–70.
[17] Baggett JC, Monro TM, Furusawa K, Finazzi V, Richardson DJ. Understanding bending losses in holey optical fibers. Opt Commun 2003;227:317–35.
[18] Sakai J, Kimura T. Bending loss of propagation modes in arbitrary-index profile optical fibers. Appl Opt 1978;17:1499–506.
[19] Mortensen NA. Effective area of photonic crystal fibers. Opt Express 2002;10:341–8.
[20] Koshiba M, Saitoh K. Structural dependence of effective area and mode field diameter for holey fibers. Opt Express 2003;11:1746–56.
[21] Gangwar R, Singh SP, Singh N. Gain optimization of a erbium-doped amplifier and two-stage gain-flattened EDFA with 45 nm flat bandwidth in the L-band. Optik 2010;121:77–9.
[22] Kogure T, Furusawa K, Lee JH, Monro TM, Richardson DJ. An erbium doped holey fiber amplifier and ring laser. Post deadline paper, Rimini, Italy, ECOC 03; 2003.
[23] Cucinotta A, Poli F, Selleri S. Design of erbium-doped triangular photonic-crystal-fiber-based amplifiers. IEEE Photon Technol Lett 2004;16:2027–9.
[24] Vershney SK, Saitoh K, Koshiba M, pal BP, sinha RK. Design of S-band erbium-doped concentric dual-core photonic crystal fiber amplifiers with ASE suppression. J Lightwave Technol 2009;27:1725–33.
[25] Temmar A, Saadi HO, Boutaleb A. Simulation based analysis of erbium doped fiber amplifier (EDFA). J Appl Sci 2006;6:789–94.
[26] Nielsen MD, Mortensen NA, Albertsen M, Folkenberg JR, Bjarklev A, Bonacinni D. Predicting macrobending loss for large-mode area photonic crystal fibers. Opt Express 2004;12:1775–9.
[27] Furusawa K, Kogure T, Monro TM, Richardson DJ. High gain efficiency amplifier based on an erbium doped aluminosilicate holey fiber. Opt Express 2004;12:3452–8.
[28] Mortensen NA, Folkenberg JR, Nielsen MD, Hansen KP. Modal cutoff and the V parameter in photonic crystal fibers. Opt Lett 2003;28:1879–81.
[29] Lizier JT, Town GE. Splice losses in holey optical fibers. IEEE Photon Technol Lett 2001;13:794–6.
[30] Corning SMF-28TM CPC6 single-mode optical fiber. Corning Incorporated Telecommunication Products Division, PI1036, ISO 9001 registered; issued on October 1998.